Werk

Jahr: 1980
Kollektion: fid.geo
Signatur: 8 Z NAT 2148:47
Digitalisiert: Niedersächsische Staats- und Universitätsbibliothek Göttingen
Werk Id: PPN1015067948_0047
PURL: http://resolver.sub.uni-goettingen.de/purl?PPN1015067948_0047

LOG Id: LOG_0022
LOG Titel: Gravity and a model of the median valley
LOG Typ: article

Übergeordnetes Werk

Werk Id: PPN1015067948
PURL: http://resolver.sub.uni-goettingen.de/purl?PPN1015067948
OPAC: http://opac.sub.uni-goettingen.de/DB=1/PPN?PPN=1015067948

Contact

Niedersächsische Staats- und Universitätsbibliothek Göttingen
Georg-August-Universität Göttingen
Platz der Göttinger Sieben 1
37073 Göttingen
Germany
Email: gdz@sub.uni-goettingen.de

J. Geophys. 47, 91–98, 1980

Journal of Geophysics

Gravity and a Model of the Median Valley

B.J. Collette, J. Verhoef, and A.F.J. de Mulder
Vening Meinesz Laboratorium, University of Utrecht, Budapestlaan 4, NL-3584 CD Utrecht, The Netherlands

Abstract. The average median valley of the Mid-Atlantic Ridge between 12° and 18° N is described as a smooth depression flanked on both sides by a high. This applies both to the bathymetry and to the gravity anomalies. This picture of the median valley and its walls was obtained by stacking profiles across the valley in 50- to 70-km-wide bands. The reduced median valley can then be interpreted as the result of the parting of the lithosphere and the response of the asthenosphere as a viscous layer to repeated unloading. Fluid dynamic equations show that the response is in general broader than the original load disturbance. We describe this as a viscous lag of the shorter wavelength components. A steady-state solution was reached by numerical methods, showing a depression accompanied by a high on both sides. For the asthenosphere under the Mid-Atlantic Ridge at these latitudes a value followed for the kinematic viscosity of 1.5×10^{19} stokes. The model can be extended to other parts of the mid-ocean ridge system by adapting the time-dependent constants (viscosity and spreading rate). If the viscosity is a factor 5 lower, no median valley results. Rising to isostatic equilibrium of a light body under the floor of the median valley then accounts for the existence of a median ridge like found at Reykjanes Ridge and at the East Pacific Rise. The coefficient of viscosity under the East Pacific Rise would be about 0.4×10^{18} stokes. The concept of a viscous lag of the short-wavelength components replaces Sleep's (1969) original notion of a 'loss of head'. The secondary valleys and ridges found in the median valley and on the flanks of the Mid-Atlantic Ridge crest cannot be explained by the model. They represent essentially a non-continuum process, in which presumably an episodic jumping of the inner valley plays an important role. Additional faulting occurs at the hinge line between the floor and the walls of the median valley.

Key words: Gravity – Median valley – Asthenosphere – Rheology – Mid-Atlantic Ridge.

Introduction

In a few consecutive surveys in the years 1975 to 1978 the Mid-Atlantic Ridge crest was surveyed between latitudes 12° and 18° N (Fig. 1). In total 55 E-W and 5 NE-SW sections were made. For the reconstruction of the 15°20′ N or Fifteen-Twenty fracture zone additional use was made of older data (Collette et al., 1974a and b; Peter et al., 1973). The measurements consisted of continuous seismic profiling, total magnetic field and gravity measurements. The tracks were controled by satellite navigation.

The present paper deals with the gravity field over the median valley and its walls. From our data it follows that the median valley is below its isostatic equilibrium position and that the walls are upheaved. This information is used for developing a model of the median valley based on fluid dynamics. The asthenosphere is treated as a viscous Newtonian fluid which reacts on the parting of the overlying lithosphere. The negative load created by this parting gives rise to a steady-state wave pattern in the underlying viscous layer. This wave accounts for the primary topography of the ridge crest. By lowering the coefficient of viscosity of the asthenosphere the mechanism can be made to yield a mid-ocean ridge crest without a median

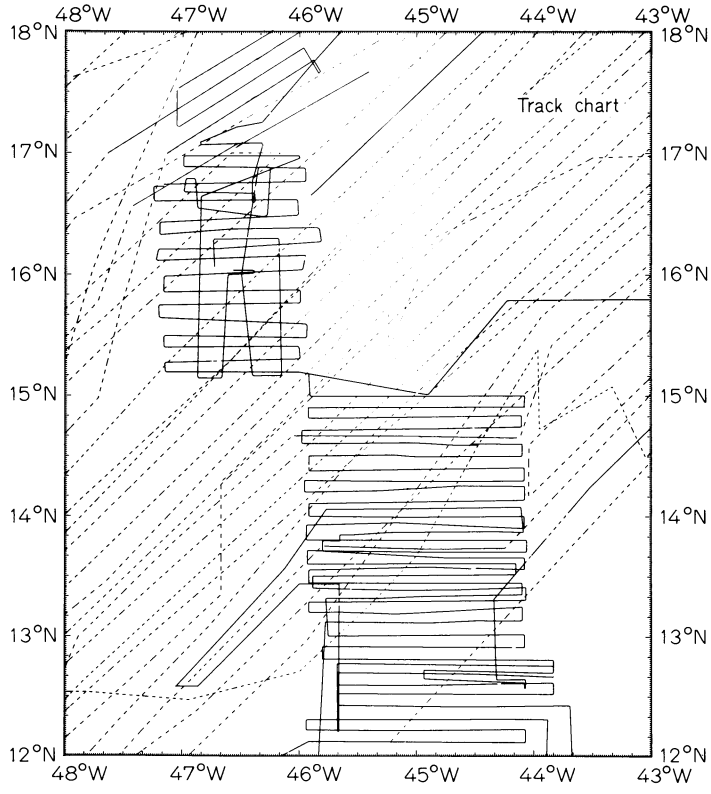

Fig. 1. Track chart. *Solid lines* are tracks of MV Aegeon Express, MV Tyro, MV Mercurius, MV Ares, and MV Marathon. *Dashes* are other tracks of the KROONVLAG-project

0340-062X/80/0047/0091/$01.60

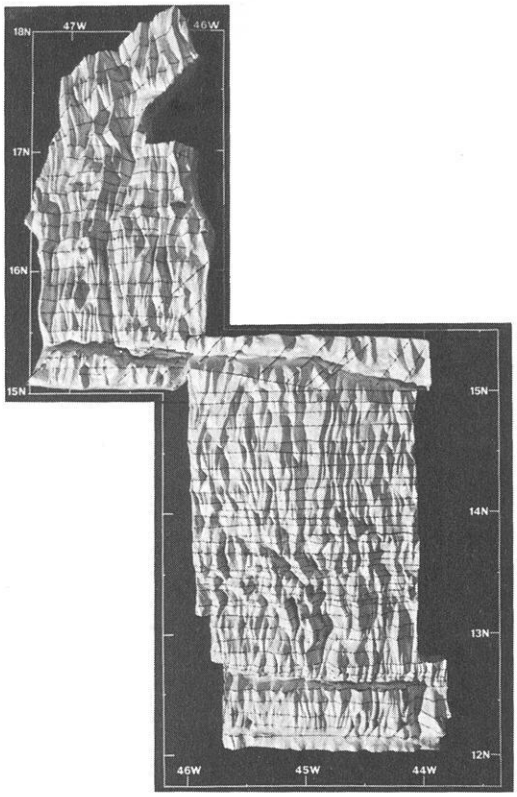

Fig. 2. Plasticine model of the Ridge Crest. Due to the light falling in from the SW, the 12°10′ fz shows less clearly

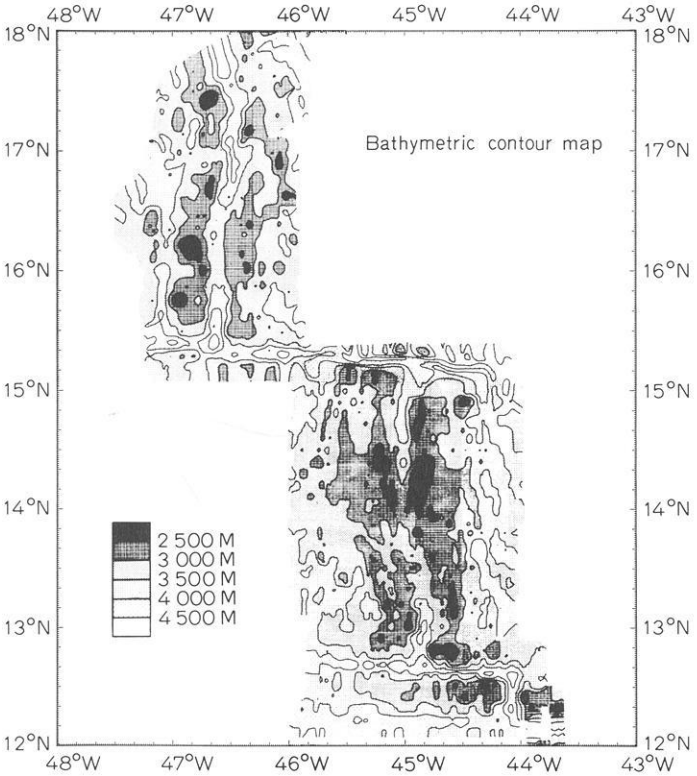

Fig. 3. Bathymetric contour map. Filter setting for the northern section $6dB/10.5$ nm, for the southern part $6dB/7.5$ nm. N–S anisotropy factor for both areas 1.5. The eastern part of the Fifteen-Twenty fz has been contoured by hand

valley, like on Reykjanes Ridge and the East Pacific Rise. A lower viscosity can be related to a higher molten fraction in the asthenosphere. The relation between a different thermal regime and the absence of a median valley was also proposed by Cochran (1979).

The secondary topography, viz. the ridges and valleys parallel to the spreading axis, cannot be accounted for by the proposed mechanism. This is essentially a non-continuum process in which we recognize two aspects: an episodic jumping of the inner valley (Collette et al., 1979) and relaxation faulting of the accreting lithosphere at the hinge line of the floor of the median valley to the walls, as described by Laughton and Searle (in press). The flexure in the lithosphere as such is caused by the steady-state wave pattern in the asthenosphere described in this paper. Our data do not contribute to the discussion whether horst and graben formation occurs at the flanks of the mid-ocean ridges, i.e., outside the median valley, as proposed by Luyendyk and Macdonald (1977).

The outcome of our study is compared with several other papers approaching the problem of the median valley and its walls from a mechanical point of view. Sleep (1969) originally introduced the effect of viscous forces in the asthenosphere using the term 'loss of head'. Sleep and Rosendahl (1979) published a study of numerical fluid dynamic models for mid-ocean ridge axes. Without explicitly saying so, these authors also arrive at the conclusion that the walls of the median valley, the lithospheric lid, are elevated above their equilibrium position by the fluid dynamic response of the asthenosphere. Lachenbruch (1976) speaks of an upward traction of the rising mantle on the adjoining lithosphere. Such an effect may be present under specific geometric conditions in addition to the vertical forces exerted on the lithosphere by the flowing asthenosphere, the steady-state wave described in this paper. Tapponnier and Francheteau (1978) relate the gravity anomalies to the effect of 'necking' of the spreading lithosphere which nevertheless would retain sufficient strength to react as an elastic plate. From the present data, we cannot exclude that this process also plays a role in the formation of the median valley.

The Topography

The topography is presented in the form of a plasticine model (Fig. 2) and a contour map (Fig. 3). The contour map is a hybrid composition of three detail maps. The northern and the southern part were produced by a computer program designed by Slootweg (1978). This method implies the use of a filter accounting for the finite spacing of the track lines. To allow for the obvious overall N–S linearity of the area, an anisotropy factor of 1.5 was introduced, thus giving more weight to this direction. The eastern part of the Fifteen-Twenty Fracture Zone was contoured by hand on the basis of older data (Collette et al., 1974a; Peter et al., 1973). Both the plasticine model and the contour map show that important deviations of the N–S linearity occur, i.e., apart from the three major fracture zones that can be recognized. The plasticine model brings out the lineations in more detail and shows alining over distances of several tens of kilometres. This alining also becomes evident from comparing adjoining sections. For showing these lineations by computer a more sophisticated program is needed which would be able to recognize slopes from the correlation between individual sections. For the time being, we still have to work with the plasticine model as an artist's impression.

The Fifteen-Twenty Fracture Zone (fz) with an offset of 165 km divides the area into two parts. To the south we further find the 12°40′ N fz and the 12°10′ N fz with offsets of 80 km and 45 km, respectively. The pattern is clearly orthogonal with local deviations of the general N–S direction of about 10 degrees. The Fifteen-Twenty fz measures 93° ± 2° with respect to the direction of the median valley, the 12°40′ N fz and the 12°10′ N fz both measure 90.0° ± 0.5°. From this we conclude that the present spreading direction is 90°. At the boundaries of the surveyed area indications can be found for the earlier sea-floor spreading direction with an azimuth of 105°. This especially applies to the non-active sections of the Fifteen-Twenty fz to the east and of the 12°40′ N fz to the west.

In addition to the large offset orthogonal fracture zones, several twists can be seen in the median valley. The most obvious ones occur at 17°40′ N, 16°40′ N, and 13°45′ N. A minor feature is found at 12°55′ N. The magnetics (W. Twigt, internal report) indicate that also at 14°45′N the N–S linearity is disturbed, though here the median valley seems not affected. The effective offset of the median valley by the 'twists' is never more than about 20 km. In a previous paper (Collette et al., 1979) we suggested that the twists are oblique transform faults or zones. We also might call them leaky transforms or narrow zones of oblique spreading. All these descriptive terms are applicable. Until recently this type of transform was not recognized as such (cf. Searle and Laughton, 1977; Rea, 1978). Searle and Laughton relate the anomalous character of these short-offset fracture zones to the circumstance that the adjoining ends of the spreading axes are physically so near that no cold zone can develop in between. We support this interpretation. The asthenospheric conduit in terms of temperature and magma supply, is evidently not interrupted by offsets which are of the same order of magnitude as that of the width of the median valley. However, the strength of the growing lithosphere is large enough to imprint its preferred faulting direction on the topography, thus influencing the course of the asthenospheric conduit. The preferred faulting direction is perpendicular to the maximum tension or the spreading direction. Oblique transforms are probably not stable. The offset would disappear by a small jumping of the spreading axis. We have the impression that such jumps indeed occur, forming one of the mechanisms that are responsible for the origin of the second-order topography. We come back to this later.

The resolution of our data is not large enough to define the exact character of the oblique fracture zones. En echelon spreading centers seem to occur at several places, of the same type as described by Ramberg et al. (1977) for the FAMOUS area, e.g. in Fracture Zone C which too has only a minor offset. Small E-W faults of the type found in FAMOUS area Fracture Zones A and B would escape our attention. In this context we refer to the clay experiments of Courtillot et al. (1974), which help to understand the type of yielding in oblique transform zones.

The question arises how oblique transform zones originate. One might think of them as the product of a primary instability of the median valley as such, caused by a haphazard jumping of sections of the spreading center, the inner valley(s). We prefer, however, the interpretation that they are caused by changes in the sea floor spreading direction. The offset of a fracture zone can be reduced considerably by a change in spreading direction to the effect that the two spreading centers (the points of intersection of the median valley segments with the fracture zone) come so close that they merge. The cold zone in between is no longer wide enough for an orthogonal fracture zone to subsist

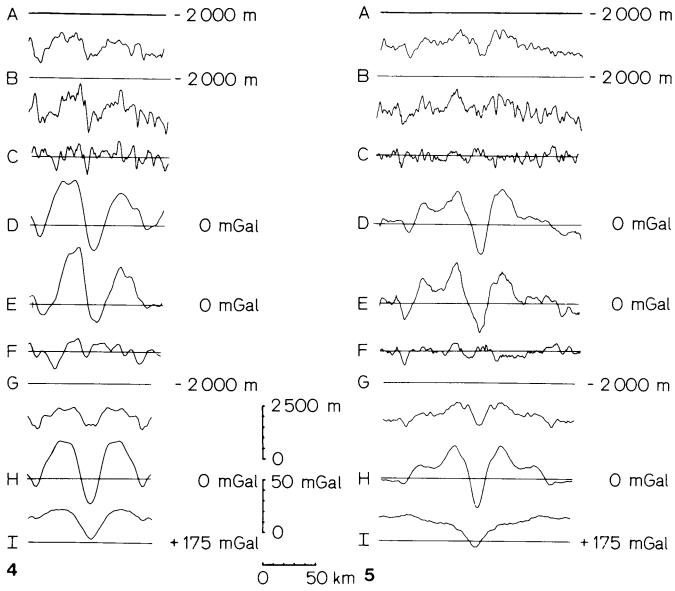

Fig. 4. *A* Stacked bathymetry for the profiles between 15°40′ and 16°25′ N. *B* Individual bathymetric profile at 16°10′ N. *C* Residual for the same profile. *D* Stacked free-air anomalies for the profiles of (*A*). *E* Free-air anomalies for the profile of (*B*). *F* Residual free-air anomalies for the same profile. *G* The stacked bathymetry symmetrized. *H* The free-air anomalies symmetrized. *I* Bouguer anomalies of the symmetrized profile

Fig. 5. *A* Stacked bathymetry for the profiles between 14°10′ and 14°40′ N. *B* Individual bathymetric profile at 14°30′ N. *C* Residual for the same profile. *D* Stacked free-air anomalies for the profiles of (*A*). *E* Free-air anomalies for the profile of (*B*). *F* Residual free-air anomalies for the same profile. *G* The stacked bathymetry symmetrized. *H* The free air anomalies symmetrized. *I* Bouguer anomalies of the symmetrized profile

and it passes into an oblique transform zone. This may explicitly be true for the oblique transform zones at 17°40′ N, at 14°45′ N (where we have only magnetic indications of a disturbance) and at 13°45′ N. An earlier reconstruction of the area (Collette et al., 1974b) postulated the existence of fracture zones at or near these latitudes. Also, the adjustment of the median valley to a new spreading direction may involve the origin of new transforms with small offsets (cf. Menard and Atwater, 1968, Fig. 5). We suppose that these new transforms are of the oblique type. In the course of time the median valley segments could straighten again by annihilation of the offsets of the oblique transforms effected by a jumping of one or both of the spreading centers involved. This jumping would not be haphazard but on the average be directed towards the warmer mid-line, thus reducing the twist in the asthenospheric conduit.

We needed this digression on oblique transform zones to account for our selection of median valley segments to be used for developing a standard model of the median valley. This standard model must define which part of the topography is 'primary', i.e., essential for the phenomenon of the median valley as such, and which part is 'secondary', varying from one place to

the other. We chose for this two areas well away from the orthogonal fracture zones and from the oblique transform zones. The first area is between 15°40′ and 16°25′ N, comprising 6 profiles, the second between 14°10′ and 14°40′ N with 5 profiles. We stacked the topography along a N–S direction and obtained the curves of Figs. 4A and 5A. The stacking procedure appears to reduce the median valley to an about 20-km-wide depression with a high to both sides. This generalized form of the median valley can also be read from the filtered contour map (Fig. 3). In the residuals we can no longer recognize a central valley (Figs. 5B and C and 6b and c). Actually, the spreading center could be any of the 'secondary' valleys. The problem of the origin of the ridge crest topography therefore falls apart into two questions:

(a) to account for the smooth curve of Figs. 4A and 5A, the reduced median valley, as a steady-state phenomenon with respect to the central axis;

(b) to explain the pseudo-linear ridges and valleys which form the secondary topography of the rift flanks and of the ocean floor in general, and which are superimposed on this smooth curve.

The Gravity Field

Figure 6 shows the contoured free air anomalies. We did not incorporate the few existing data over the eastern part of the Fifteen-Twenty Fracture Zone. Since the gravity field is much smoother than the topography, the effect of filtering (same procedure as for the topography but with isotropic filtering) is far less. The contours are reasonably parallel in the two areas chosen for the model. Figures 4D and 5D give the stacked anomaly curves for these areas, using the same profiles as for the topography. Figures 4E and 5E give two individual gravity profiles, Figs. 4F and 5F the residuals for these sections, i.e., the anomalies after subtraction of the stacked curves.

The stacked curves of Figs. 4 and 5 still show the effect of some large valleys that are found to the west and east of the median valley, in Fig. 4 at a distance of 55 km and in Fig. 5 at 70 km. We consider these valleys as incidental features occurring in these special sections of the ridge and not specific for the history of sea-floor spreading in the area as a whole. However, since such hazards still may influence our starting point, we cannot attach too much value to the way the positive anomalies fall back to zero on the flanks. In addition, we have to bear in mind that the zero level needs further definition. Cochran and Talwani (1977) demonstrated that in general a regional positive free-air anomaly of the order of 30 mGal exists over mid-ocean ridges. In view of the circumstance that the mean anomaly is +14 mGal in the nothern part and +6 mGal in the southern part, the area as a whole must be regarded as negative (cf. Cochran and Talwani, 1978). We will not dwell on this aspect here.

In Figs. 4G and H and 5G and H we symmetrized the stacked topography and the stacked free-air anomalies by averaging both sides. Next we computed the Bouguer anomalies for these profiles with densities ranging from 2.5 to 2.9 g cm^{-3}. The smoothest curves were obtained with densities 2.5 and 2.6 g cm^{-3}. Figures 4I and 5I give the results with 2.5 g cm^{-3}. The curves differ since the southern survey covers a broader area. Figure 5I therefore shows more of the regional effect of the isostatic compensation of the ridge. Talwani et al. (1965; cf. Talwani, 1970, Fig. 16) showed that the isostatic compensation is situated in the upper mantle, i.e., in the asthenosphere. Since the asthenosphere

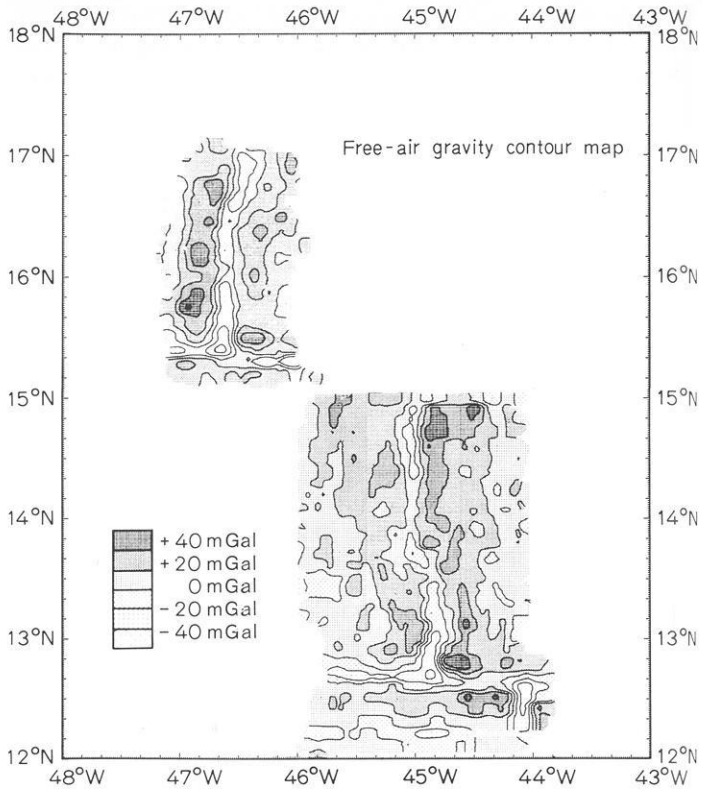

Fig. 6. Free air anomaly contour map. Filter setting is the same as for Fig. 3. No anisotropy factor applied

cannot statically bear the involved stress, this configuration does not represent a real equilibrium and can only be explained in terms of sea-floor spreading. The asthenosphere is less dense under the ridge than farther away which may be attributed to a larger molten fraction.

Since in this study we are only interested in the short wavelength components of the gravity field, we have to subtract the 'regional' from the Bouguer anomaly curves. This regional is ill-defined. Nevertheless, we can isolate a negative anomaly under the median valley which can only be caused by a shallow body. The anomaly can be modelled by a two-dimensional body of rectangular cross-section immediately beneath the surface, with a density contrast of $-0.15\,g\,cm^{-3}$ and which is 12 km wide and 14 km deep, on both sides accompanied by a body with a density contrast of $+0.15$ g cm^{-3}, with its top at 7 km and its bottom at 9 km depth beneath sea-level and between 12 and 24 km from the axis. As always with gravity anomalies, other solutions are possible but they all have in common that the walls of the median valley are not compensated locally. The geometry of the light body causing the central negative anomaly is corroborated by seismic results obtained in the Famous area (Fowler, 1976).

Model of the Median Valley

From Figs. 4G and I and 5G and I we derived a total vertical load curve by adding the anomalous subsurface masses to the masses of the averaged bathymetric stacks. The resulting curve is given as Fig. 7a. This curve is taken to represent the load on an otherwise free surface of a viscous fluid layer of thickness h. This

load can be considered to consist of a negative part, due to the separation of the lithosphere which creates a gap, and the positive and more regional response of the asthenosphere to this. The configuration is much like the idea of regional isostatic compensation with an elastic lithosphere. However, now it is not a static elastic problem, but a dynamic viscous one.

The hydrodynamic equations for dealing with this can be found in Burgers and Collette (1958). They arrived at the following expression for the decay of a two-dimensional sinusoidal wave of small amplitude z_0 and wavelength $2\pi/a$ at the surface of a viscous fluid

$$z = z_0 \exp(-kt)\cos(ax) \tag{1}$$

in which k is a decay constant, equalling

$$k = \frac{g}{2va} \tag{2a}$$

for an infinite halfspace (g being the acceleration of gravity and v the coefficient of viscosity) and

$$k = \frac{g}{2va} \cdot \frac{\cosh(ah)\cdot\sinh(ah) - ah}{\cosh^2(ah) + (ah)^2} \tag{2b}$$

for a layer with thickness h.

If we next express the surface load disturbance $p(x,0) = \rho g z(x,0)$ (ρ being the density) as a Fourier series with

$$z(x,0) = C_o + \sum_{n=1}^{N} C_n \cdot \cos\frac{n\pi x}{L}, \tag{3a}$$

the deformation of the surface as a function of t becomes

$$z(x,t) = C_o + \sum_{n=1}^{N} C_n \cdot \exp\left(-\frac{k' t}{n}\right) \cdot \cos\frac{n\pi x}{L}. \tag{3b}$$

In these expressions $2L$ is the interval at which the surface load disturbance repeats itself. This interval was chosen at 2,000 km in our computations. The decay constant k' becomes

$$k' = \frac{gL}{2\pi v} \tag{4a}$$

for an infinite halfspace, and

$$k' = \frac{gL}{2\pi v} \cdot \frac{\cosh(n\pi h/L)\cdot\sinh(n\pi h/L) - n\pi h/L}{\cosh^2(n\pi h/L) + (n\pi h/L)^2} \tag{4b}$$

for a layer with thickness h.

From here we proceeded as follows. Different forms for the surface load $p(x,0)$ were taken, ranging from a narrow gap via a rectangular form to a smooth identation for which we took a Gauss function. Then the form of the surface after a time dt was computed with Eq. (3b). In principle this form consists of a broad positive bulge superimposed on the initial disturbance. Next a new load of the same initial form was added and the resulting form of the surface after a time $2\,dt$ was computed, and so on. The results best resembling Fig. 7a were obtained with the Gauss function

$$z(x,0) = z_o \cdot \exp\left(-\frac{x^2}{a_o^2}\right). \tag{5a}$$

The halfwidth of this function is

$$d = (-\ln 0.5)^{\frac{1}{2}} a_o = 0.83\, a_o. \tag{5b}$$

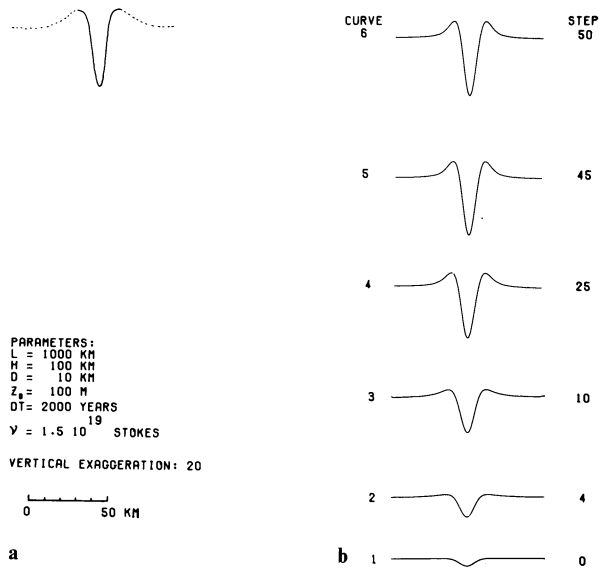

Fig. 7. a Load curve derived from Figs. 4 and 5. **b** Steady-state solution *(Curve 6)* for a periodically renewed negative load *(Curve 1)*. *Curves 2 to 5* give intermediate stages

The solution could be made steady state in a fairly rapid way by choosing the right value of v (see Fig. 7b). The convergence of the method can be proved for an infinite halfspace. For a layer with finite thickness h the convergence cannot be proven rigorously, but follows indirectly since the effect of h is only important for a finite number of terms, the long wavelength components. This implies that for reasonable values of h the method remains valid.

The amplitude of the resulting curve, the steady state solution, depends on v and on the ratio z_o/dt. This ratio forms together with a_o a measure for the bulk of the flow involved. The value of h appeared not to be critical. The largest effects of varying h occur in the outward flank of the positive bulge, a part of the experimental curve which is ill-defined as mentioned before. For h a value of 100 km was taken.

Discussion of the Model

At this point the spreading velocity enters the discussion. For this we have to quantify the renewal of the initial indentation. If the lithosphere is moved apart over a distance of $2dx$, we have to consider three aspects:

1. the creation of a gap along the central axis,
2. the viscous drag of the lithosphere on the asthenosphere while moving, and
3. the accretion of the lithosphere over a much broader area.

This accretion equals the difference between two cooling curves for the oceanographic lithosphere, which are mutually shifted over a distance dx. This difference consists only of very long wavelengths.

The short-wavelength gravity data describe only the first two aspects, the parting of the lithosphere along the central axis and the drag of the lithosphere on the asthenosphere. If we take the thickness of the lithosphere at the ridge crest at 10 km, the first effect is $10^6 \times b\,\mathrm{cm}^2/\mathrm{a}$, if b is the spreading velocity (halfrate).

The flow needed to balance the drag of the lithosphere on the asthenosphere is half the thickness of the asthenosphere h times the spreading rate. Again putting h at 100 km, this flow equals $5 \times 10^6 \times b\ \mathrm{cm}^2/\mathrm{a}$.

We now make the following assumptions:

(a) a non-viscous process which might be called 'necking' after Tapponnier and Francheteau (1978) transforms the gap at the ridge crest into a shallow indentation;

(b) the horizontal drag exerted by the lithosphere on the asthenosphere creates also a depression near the axis (a very crude description, but sufficient for the present purpose); and

(c) the sum of both effects can be described by a Gauss function with halfwidth $d = 0.83\, a_o$.

With these assumptions the relation between the spreading velocity b and the bulk of the flow expressed in z_o/dt and a_o becomes

$$6\ \ 10^6\ \ b\,\mathrm{cm}^2/\mathrm{a} = \frac{z_o}{dt} \int_0^\infty \exp\left(-\frac{x^2}{a_o^2}\right) dx\,\mathrm{cm}^2/\mathrm{a}. \qquad (7)$$

The value of the integral of (7) is 10.6×10^{10} if we take d at 10 km. This gives

$$\frac{z_o}{dt} = 5.66 \times 10^{-5} \times b.$$

This value was used to estimate v. b was taken at 1 cm/a, z_o at 0.1 km and dt at 2,000 a. Different values of v were tried. With $v = 1.5 \times 10^{19}$ stokes the steady state curve has an amplitude of 975 m. This is considered a fair approach of the experimental curve of the median valley. The steady state solution was reached in 50 steps (change in peak-to-peak amplitude of the last step well within 0.5 %).

Reykjanes Ridge and East Pacific Rise

The model can be extended to explain the different physiography of other parts of the mid-ocean ridge system like Reykjanes Ridge and the East Pacific Rise by adjusting the time dependant parameters, viscosity v and spreading rate b. If the effective viscosity is diminished by a factor 5, no appreciable median valley results. This might apply to the configuration of Reykjanes Ridge where the median valley gradually disappears going north to change into a positive topographic feature (Talwani et al., 1971; Laughton et al., 1979). The positive topography can be explained by a rise to isostatic equilibrium of the light material which, according to Figs. 4 and 5, is found in a narrow zone under the median valley, or more correctly, the spreading axis. If the spreading rate is increased by a factor 5, we again obtain the configuration of Fig. 7b. This means that in order to explain the positive topography of the East Pacific Rise we have to lower the effective viscosity again by the appropriate factor. The viscosity there would then be about 0.4×10^{18} stokes.

The correlation of a low viscosity with a larger molten fraction of the asthenosphere is readily made in both cases. The observations on profuse volcanism (R.D. Ballard, personal communication) on the East Pacific Rise are direct evidence for this as well as the abundant volcanism on Iceland. A larger molten fraction does not mean that the temperature would necessarily be higher. Instead the heat content (or the Helmholtz free energy) would be higher under the East Pacific Rise and under Reykjanes Ridge than under the Mid-Atlantic Ridge.

Origin of the Secondary Topography

The gravity data thus yield a clue to the mechanism that is responsible for the presence or absence of the median valley. For the explanation of the secondary ridges and valleys that are found at the ridge crest, the residuals of Figs. 4C and 5C, we turn our attention to the plasticine model of Fig. 2. It appears that the secondary topography *in* the median valley (which is defined by the curve of Fig. 7a) and *on* the flanks is essentially the same, i.e., on this scale and with this resolution. It therefore seems reasonable to conclude that the secondary topography originates in the median valley as originally proposed by Needham and Francheteau (1974). This could be effectuated by an episodic jumping of the actual spreading axis, the inner valley. Considering the en echelon character of the inner valley at places, which as such cannot be a steady state configuration, a jumping of the inner valley seems plausible. The mean mutual distance between the secondary valleys (about 6 km) against a spreading rate of 1 cm/a then tells us that such a jumping takes place every $6 \cdot 10^5$ a on the average (Collette et al., 1979).

The secondary topography is furthermore affected by the faulting which takes place at the hinge line of the median valley floor and the walls. Laughton and Searle (in press; see also Searle and Laughton, 1977) describe this faulting for four different sections of the Mid-Atlantic Ridge. The faults have a typical spacing of 2 to 2.5 km, equivalent to initiation of a new fault about every 2×10^5 a. According to their data, reduction of the effective vertical throw of the faults is realized by a rotation of the blocks between the consecutive faults once they have been transported over the crest of the wall of the median valley. This is contrary to the interpretation of Luyendyk and Macdonald (1977) who suppose that the reduction is realized by another faulting process with faults facing outward from the spreading axis. This would result in a horst/graben formation at the flanks. The resolution of our data is not such that they can contribute to the discussion. All we can say is that in our concept there is no actual need for additional horst/graben formation on the flanks.

General Discussion

Sleep and Rosendahl (1979) recently presented a study of numerical fluid dynamic models of mid-ocean ridge axes. These authors take also the temperature dependance of the coefficient of viscosity into account (see also Sleep, 1975). Furthermore they introduce the effect of a magma chamber, a small one for slow spreading ridges and a large one for fast spreading ridges. The introduction of this effect makes it possible to model also such details as asymmetric spreading. However, we doubt whether this is realistic in view of the occurrence of non-continuum processes. This puts restrictions to the applicability of any steady state model including ours. Apart from that, their result is very similar to ours. The outcome of our computations then proves that the origin of the median valley with its elevated walls is not dependant on the existence of a 'conduit' or a magma chamber, but follows directly from the rheology of the asthenosphere as a horizontal viscous layer. The original, rather loosely defined concept of a 'loss of head' by Sleep (1969; see also Sleep and Biehler, 1970) may now be written more precisely as a 'viscous lag' of the short wavelength components of a (continuously renewing) disturbance.

In the approach by Lachenbruch (1973, 1976) the concept of a conduit plays an overall important role. Lachenbruch arrived

at an upward traction of the upwelling viscous mantle on the solid(ifying) walls of the conduit, the lithosphere. If the conduit walls are steep, a bottleneck effect may indeed become important. Further computations are necessary to estimate the effect of different shapes of the upper surface of the viscous layer on the response function to a load disturbance.

An entirely different mechanical approach to the problem of the median valley and its walls is given by Tapponnier and Francheteau (1978), to which paper we referred earlier when discussing the mechanism by which the hypothetical 'gap' in the lithosphere is transformed into a smoother load disturbance at the boundary between lithosphere and asthenosphere. We supposed that this was realized by a non-viscous thinning of the lithosphere, called 'necking' by Tapponnier and Francheteau. However, the authors go further and describe the effect of the thinning of the lithosphere as a negative loading on an elastic plate which reacts with a regional upwarping according to the theory developed by Vening Meinesz (Heiskanen and Vening Meinesz, 1958). Essentially, the authors thus treat the problem as pseudo-static, in contrast to a fluid dynamic approach. The following comment can be made. Since both the static elastic solution and the fluid dynamic approach lead to a same result, it is not possible to distinguish between them in an empirical way. Also on theoretical grounds, it is difficult to make an exclusive choice. The accreting lithosphere, however weak, will have some elasticity and the assumptions of Tapponnier and Francheteau with regard to Young's modulus and to the thickness of the viscoelastic lithosphere, are not excessive. For the time being, we therefore cannot decide how the two processes interrelate and whether elastic upwarping indeed contributes in a material way to the phenomenon of a depressed median valley accompanied by elevated walls.

Finally, we mention a study by Cochran (1979) who made an analysis of the gravity field over the mid-ocean ridge crest on a worldwide basis. This author describes the relation between gravity and bathymetry in the form of a filter obtained by cross-spectral techniques. The interpretation of the filter is entirely static in terms of the response of a thin elastic plate overlying a weak fluid. The best fitting elastic thickness to explain gravity and bathymetry then is 7 to 13 km for the Mid-Atlantic Ridge and 2 to 6 km for the East Pacific Rise and for Reykjanes Ridge. Cochran relates this difference to different temperature structures under these ridges. Essentially, Cochran's approach is thus the same as the one by Tapponnier and Francheteau and the same comment can be made. With regard to the filter method as such, we want to point out that the interpretation may disguise certain features like the presence of low density bodies under the spreading axis. The extreme low surface density of $2.3\,g\,cm^{-3}$, which followed from the interpretation of the East Pacific Rise filter, may result from this.

Conclusions

The outcome of the study of the gravity field over the Mid-Atlantic Ridge crest between 12° and 18° N can be summarized as follows.

1. The median valley is characterized by a negative free-air anomaly. This anomaly finds its source partly in the topography and, for another part, in a light body under the floor of the median valley. The walls of the median valley are accompanied by positive anomalies which can be explained partly by the direct topographic effect and, for a smaller part, by the upheaved position of the walls. In terms of gravity, the median valley can thus be described as a depressed zone, accompanied on both sides by elevated zones.

2. Alternatively, one can describe this configuration as a negative anomaly superimposed on a broader positive anomaly. The broad positive anomaly then can be considered as the response of the asthenosphere (upwarping) to a continuously renewing negative load. This renewed loading is the effect from the parting of the lithosphere in the oceanfloor spreading process.

3. The upwarping can be reproduced in a steady-state model by using the fluid dynamic equations for a viscous layer. The regional upwarping results from the circumstance that the decay time of a sinusoidal wave is inversely proportional to its wavelength. Hence short wavelength components of a disturbance have a longer decay-time than long wavelengths. This leads to a systematic viscous lag of the short wavelengths components.

4. The coefficient of viscosity v of the asthenosphere under the Mid-Atlantic Ridge is 1.5×10^{19} stokes with an assumed thickness of the asthenosphere of 100 km.

5. The model can be extrapolated to Reykjanes Ridge and the East Pacific Rise by lowering the viscosity. If the viscosity is reduced by a factor 5, the depression or median valley disappears. The light body under the floor of the median valley will also try to reach its equilibrium position, which gives positive topography or a median ridge. If the spreading rate becomes larger, this effect is undone. The foregoing means that the effective viscosity of the asthenosphere under Reykjanes Ridge must be about 5 times lower and under the East Pacific Rise about 40 times lower than under the Mid-Atlantic Ridge.

6. The secondary topography, i.e., the ridges and valleys parallel to the median valley on the ridge flanks and, in general, in the ocean floor, can best be explained as resulting from an episodic jumping of the inner valley. The data suggest that such a jumping takes place about every 6×10^5 a. In addition, the young lithosphere is faulted along the hinge line between floor and wall of the median valley when transported uphill (every 2 km or 2×10^5 a, as concluded by Searle and Laughton, 1977).

7. The results are in agreement with model studies by Sleep and Rosendahl (1979). Our concept of a 'viscous lag' of the short wavelength components of a disturbance replaces Sleep's original notion (1969) of a 'loss of head'. A bottleneck effect may be present and add to the upwarping (Lachenbruch, 1976). Also elastic upwarping of the lithosphere in response to a local thinning in and near the median valley, or 'necking' as described by Tapponnier and Francheteau (1978), may form part of the mechanism.

Acknowledgments. The investigations in 1975 and 1977 were carried out on board of MV Aegeon Express and MV Tyro. These ships were chartered on the account of the Netherlands Commission for Sea Research of the Royal Netherlands Academy of Arts and Sciences as part of the project VAARPLAN 1974–1978. Additional measurements were made on board of MV Ares and MV Mercurius of the Royal Netherlands Steamship Company as part of the KROONVLAG-project. This project was sponsored by the Netherlands organization for the advancement of pure science (ZWO). We thank the Royal Netherlands Steamship Company for its continued assistance to our research. Special thanks goes to the crews of the ships for their cooperation. A.P. Slootweg and P.J. de Vrijer built the cross-coupling computer that was used in 1975, before the original GSS2 Graf

Askania gravity meter was renovated by Bodenseewerk Geosystem GmbH and converted into a KSS5 system. From the students who assisted with the measurements we mention P.J. de Vrijer, C.G. Langereis, and J.W.G. Peeters who processed the gravity data.

References

Burgers, J.M., Collette, B.J.. On the problem of the post-glacial uplift of Fennoscandia. Proc. K. Ned. Akad. Wet. Ser. B: **61**, 221–241, 1958

Cochran, J.R.: An analysis of isostasy in the world's oceans: Part 2. Mid-Ocean Ridge crests. J. Geophys. Res. **84**, 4713–4729, 1979

Cochran, J.R., Talwani, M.. Free-air gravity anomalies in the world's oceans and their relationship to residual elevation. Geophys. J. R. Astron. Soc. **50**, 495–552, 1977

Cochran, J.R., Talwani, M.: Gravity anomalies, regional elevation, and the deep structure of the North Atlantic. J. Geophys. Res. **83**, 4907–4924, 1978

Collette, B.J., Rutten, K., Schouten, H., Slootweg, A.P.: Continuous seismic and magnetic profiles over the Mid-Atlantic Ridge between 12° and 18° N. Mar. Geophys. Res. **2**, 133–141, 1974a

Collette, B.J., Schouten, H., Rutten, K., Slootweg, A.P.: Structure of the Mid-Atlantic Ridge province between 12° and 18° N. Mar. Geophys. Res. **2**, 143–179, 1974b

Collette, B.J., Slootweg, A.P., Twigt, W Mid-Atlantic Ridge crest topography between 12° and 15° N. Earth Planet. Sci. Lett. **42**, 103–108, 1979

Courtillot, V., Tapponnier, P., Varet, J.: Surface features associated with transform faults: a comparison between observed examples and an experimental model. Tectonophysics **24**, 317–329, 1974

Fowler, C.M.R.: Crustal structure of the Mid-Atlantic ridge crest at 37° N. Geophys. J. R. Astron. Soc. **47**, 459–491, 1976

Heiskanen, W.A., Vening Meinesz, F.A. The earth and its gravity field., New York: McGraw-Hill 1958

Lachenbruch, A.H.: A simple mechanical model for oceanic spreading centers. J. Geophys. Res. **78**, 3395–3417, 1973

Lachenbruch, A.H.. Dynamics of a passive spreading center. J. Geophys. Res. **81**, 1883–1902, 1976

Laughton, A.S., Searle, R.C.. Tectonic Processes on Slow Spreading Ridges. 2nd Maurice Ewing Symposium, Am. Geophys. Union in press, 1979

Laughton, A.S., Searle, R.C., Roberts, D.G.. The Reykjanes Ridge crest and the transition between its rifted and non-rifted regions. Tectonophysics **55**, 173–179, 1979

Luyendyk, B.P., Macdonald, K.C.: Physiography and structure of the inner floor of the FAMOUS rift valley: Observations with a deep-towed instrument package. Bull. Geol. Soc. Am. **88**, 648–663, 1977

Menard, H.W., Atwater, T.: Changes in direction of sea-floor spreading. Nature **219**, 463–467, 1968

Needham, H.D., Francheteau, J.: Some characteristics of the rift valley in the Atlantic Ocean near 36°48′ North. Earth Planet. Sci. Lett. **22**, 29–43, 1974

Peter, G., Merrill, G., Bush, S.: Caribbean Atlantic Geotraverse. NOAA-IDOE 1971, Report No. 1, Project Introduction. Bathymetry, 1973

Ramberg, I.B., Gray, D.F., Raynolds, R.G.: Tectonic evolution of the FAMOUS area of the Mid-Atlantic Ridge, lat 35° 50′ to 37° 20′ N. Bull. Geol. Soc. Am. **88**, 609–620, 1977

Rea, D.K. Spreading-center offsets that are not transform faults. Eos. **59**, 370, 1978

Searle, R.C., Laughton, A.S.: Sonar studies of the Mid-Atlantic Ridge and Kurchatov Fracture Zone. J. Geophys. Res. **82**, 5313–5328, 1977

Sleep, N.H.: Sensitivity of heat flow and gravity to the mechanism of sea-floor spreading. J. Geophys. Res. **74**, 542–549, 1969

Sleep, N.H.: Formation of oceanic crust: some thermal constraints. J. Geophys. Res. **80**, 4037–4042, 1975

Sleep, N.H., Biehler, S.: Topography and tectonics at the intersections of fracture zones with central rifts. J. Geophys. Res. **75**, 2748–2752, 1970

Sleep, N.H., Rosendahl, B.R.: Topography and tectonics of mid-oceanic ridge axes. J. Geophys. Res. **84**, in press, 1979

Slootweg, A.P.: Computer contouring with a digital filter. Mar. Geophys. Res. **3**, 401–405, 1978

Talwani, M.: Gravity. In: The sea, vol. **4** Part 1, A.E. Maxwell, ed.: pp. 251–297. New York: Wiley-Interscience 1970

Talwani, M., Le Pichon, X., Ewing, M.. Crustal structure of mid-ocean ridges. 2. Computed model from gravity and seismic refraction data. J. Geophys. Res. **70**, 341–352, 1965

Talwani, M., Windish, C.C., Langseth, M.G., Jr.: Reykjanes ridge crest: A detailed geophysical study. J. Geophys. Res. **76**, 473–517, 1971

Tapponnier, P., Francheteau, J.. Necking of the lithosphere and the mechanics of slowly accreting plate boundaries. J. Geophys. Res. **83**, 3955–3970, 4497, 1978

Received May 16, 1979; Revised Version July 19, 1979